molecular pharmaceutics

ARTICLE

pubs.acs.org/molecularpharmaceutics

Hepatocellular Carcinoma Cells and Their Fibrotic Microenvironment Modulate Bone Marrow-Derived Mesenchymal Stromal Cell Migration *in Vitro* and *in Vivo*

Mariana G. Garcia,[†,‡,§] Juan Bayo,[†,§] Marcela F. Bolontrade,[‡,∥] Leonardo Sganga,[∥] Mariana Malvicini,[†] Laura Alaniz,[†,‡] Jorge B. Aquino,[†,‡] Esteban Fiore,[†] Manglio M. Rizzo,[†] Andrés Rodriguez,[†] Alicia Lorenti,[⊥] Oscar Andriani,[#] Osvaldo Podhajcer,[‡,∥] and Guillermo Mazzolini*[,†,‡,#]

[†]Gene Therapy Laboratory, School of Medicine, Austral University, Av. Presidente Perón 1500, (B1629ODT) Derqui-Pilar, Buenos Aires, Argentina

[‡]CONICET (Consejo Nacional de Investigaciones Científicas y Técnicas), Buenos Aires, Argentina

[∥]Laboratory of Molecular and Cellular Therapy, Fundación Instituto Leloir, Patricias Argentinas 435, (C1405BWE) Buenos Aires, Argentina

[⊥]Clinical Translation Unit, Austral University, Av. Presidente Perón 1500, (B1629ODT) Derqui-Pilar, Buenos Aires, Argentina

[#]Liver Unit, Austral University, Av. Presidente Perón 1500, (B1629ODT) Derqui-Pilar, Buenos Aires, Argentina

Supporting Information

ABSTRACT: Hepatocellular carcinoma (HCC) is the fifth most common cancer and the third cause of cancer-related death. Fibrogenesis is an active process characterized by the production of several proinflammatory cytokines, chemokines and growth factors. It involves the activation of hepatic stellate cells (HSCs) which accumulate at the site of injury and are the main source of the extracellular matrix deposits. There are no curative treatments for advanced HCC, thus, new therapies are urgently needed. Mesenchymal stromal cells (MSCs) have the ability to migrate to sites of injury or to remodeling tissues after *in vivo* administration; however, in several cancer models they demonstrated limited efficacy to eradicate experimental tumors partially due to poor engraftment. Thus, the aim of this work was to analyze the capacity of human MSCs (hMSCs) to migrate and anchor to HCC tumors. We observed that HCC and HSCs, but not nontumoral stroma, produce factors that induce hMSC migration *in vitro*. Conditioned media (CM) generated from established HCC cell lines were found to induce higher levels of hMSC migration than CM derived from fresh patient tumor samples. In addition, after exposure to CM from HCC cells or HSCs, hMSCs demonstrated adhesion and invasion capability to endothelial cells, type IV collagen and fibrinogen. Consistently, these cells were found to increase metalloproteinase-2 activity. *In vivo* studies with subcutaneous and orthotopic HCC models indicated that intravenously infused hMSCs migrated to lungs, spleen and liver. Seven days post-hMSC infusion cells were located also in the tumor in both models, but the signal intensity was significantly higher in orthotopic than in subcutaneous model. Interestingly, when orthotopic HCC tumors where established in noncirrhotic or cirrhotic livers, the amount of hMSCs localized in the liver was higher in comparison with healthy animals. A very low signal was found in lungs and spleens, indicating that liver tumors are able to recruit them at high efficiency. Taken together our results indicate that HCC and HSC cells produce factors that efficiently induce hMSC migration toward tumor microenvironment *in vitro* and *in vivo* and make MSCs candidates for cell-based therapeutic strategies to hepatocellular carcinoma associated with fibrosis.

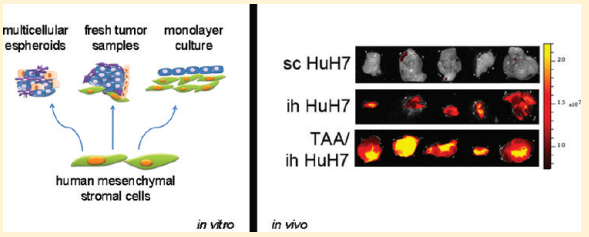

KEYWORDS: hepatocellular carcinoma, human mesenchymal stromal cells, activated hepatic stellate cells, migration

INTRODUCTION

Hepatocellular carcinoma (HCC) is the fifth most common malignancy and represents the third cause of cancer-related death worldwide.[1] The incidence and mortality associated with HCC are increasing steadily mainly due to the spreading of the epidemic hepatitis C virus infection.[2] Liver transplantation and surgical resection are curative therapies that can only be applied to a minority of patients.[1] Recently, sorafenib, a multikinase inhibitor, was approved for patients with advanced HCC and showed limited survival benefits in comparison with placebo in a phase III clinical trial.[3] Therefore, there is an urgent need for novel therapies for patients with advanced HCC. Gene and cell

Special Issue: Emerging Trends in Gene- and Stem-Based Combination Therapy

Received: March 17, 2011
Accepted: July 19, 2011
Revised: July 11, 2011
Published: July 19, 2011

dx.doi.org/10.1021/mp200137c | *Mol. Pharmaceutics* 2011, 8, 1538–1548

therapy have emerged as promising strategies to deliver therapeutic genes to tumoral or peritumoral tissues; however, poor correlation was found between responses achieved in clinical setting compared to experimental tumor models.[4,5] In this scenario, stem cells have been used as carriers to deliver antitumoral genes into tumors with promising results.[6−8] Particularly, the use of human adult bone marrow-derived mesenchymal stromal cells (hMSCs) has many potential clinical applications due to their abundance and accessibility. In addition, they are easily genetically manipulated and show great capacity to migrate toward injured or remodeling tissues after *in vivo* administration.[9] It has been demonstrated that MSCs possess tropism for experimental tumors,[6,10,11] however, evidence indicates that *in vivo* homing and engraftment depends not only on MSC intrinsic properties but also on stimuli produced by the tumor microenvironment.[12]

Liver fibrosis is characterized by an excessive accumulation of extracellular matrix (ECM) components that finally leads to liver failure.[13] Fibrogenesis is the result of chronic liver damage caused mainly by chronic hepatitis C or B virus infection and alcohol abuse.[14] The initial stage is characterized by apoptosis of hepatocytes with production of reactive oxygen species;[15] the inflammatory process leads to activation of fibrogenic cells such as hepatic stellate cells (HSCs), which in turn migrate and accumulate at the sites of tissue injury, secreting large amounts ECM proteins, proinflammatory cytokines, chemokines and growth factors such as TGF-β, TNF-α, PDGF and IGF-1.[16]

Tumors can be consider as unresolved wounds,[17] and similarly to cirrhosis, a tumor's microenvironment is characterized by an increased local production of inflammatory mediators and chemoattractants.[18] In particular, HCC produces cytokines and chemokines such as IL-6, IL-10, IFN-γ, VEGF, HGF, IGF-1, CXCL12 or SDF-1 and CCL20,[19−23] and some of them have been shown to attract MSCs.[24]

It is presumed that MSCs actively migrate toward tissues using leukocyte-like cell-adhesion and transmigration mechanisms. Thus, hMSC rolling might eventually be mediated by the interaction of selectins expressed by them as well as by inflamed endothelial cells, and the interaction of selectins with their ligands such as P-selectin glycoprotein ligand 1 (PSGL1), CD44 and E-selectin ligand 1 (ESL1) would enable them to adhere to inflamed endothelium. Integrins are transmembrane proteins known to participate in cellular rolling, which might mediate rapid arrest of hMSCs in the presence of inflammatory induced chemokines. The final step would be transmigration through the postcapillary vein walls into the tissue, a process that subsequently involves penetration of the endothelial-cell layer, the endothelial-cell basement membrane (composed by type IV collagen and laminin), and the pericytic sheath.[25]

Several strategies have been explored to deliver therapeutic genes to several tumors using hMSCs as carriers; however, limited efficacy has been demonstrated, possibly due to inability of hMSCs to target tumor/peritumoral tissues with efficacy.[26] Thus, the aim of this work was to *in vitro* and *in vivo* study hMSC migration and anchorage to human HCC. In addition, hMSC migratory responses toward different conditioned media (CM) derived from HCC and HSC cell lines as well as from patient tumor samples were analyzed. We have herein shown evidence of specific and significant recruitment of hMSCs toward HCC in *in vitro* and *in vivo* models suggesting a potential use for these cells as carriers of factors against this tumor type.

MATERIAL AND METHODS

Cell Lines. PLC/PRF/5, HuH7, and Hep3B (human HCC cell lines) were kindly provided by Prof. Jesus Prieto (CIMA, University of Navarra, Pamplona, Spain), HT-1080 (human fibrosarcoma cell line) was kindly provided by Dr. R. Daniel Bonfil (Wayne State University, School of Medicine, Detroit, MI, USA), and WI-38 (human fibroblast cell line) was obtained from the American Type Culture Collection. LX-2 cell line (human HSCs generated by spontaneous immortalization in low serum conditions) was kindly provided by Dr. Scott Friedman (Division of Liver Diseases, Mount Sinai School of Medicine, New York, NY, USA). Human microvascular endothelial cells (HMEC-1) were provided by CDC (Centers for Disease Control, Atlanta, GA, USA). Cell lines were cultured in complete DMEM (2 μmol/L glutamine, 100 U/mL penicillin, 100 mg/mL streptomycin and 10% heat-inactivated fetal bovine serum (FBS)).

Isolation of hMSCs. Cells were obtained from allogeneic bone marrow transplantation of healthy donors after informed consent (Hospital Naval Pedro Mallo, Buenos Aires, Argentina). Briefly, mononuclear cells collected from the interface of a Ficoll−Hypaque density gradient (Sigma-Aldrich) were plated in complete DMEM low glucose (Invitrogen/Life Technologies) supplemented with 20% FBS (Internegocios S.A., Argentina). After a 2 h incubation, nonadherent cells were removed by washing with phosphate-buffered saline (PBS) and adherent hMSCs were cultured and used for different experiments at passages 4 to 6. Phenotype characteristics of hMSCs were determined by flow cytometry with anti-human PE conjugated antibodies against HLA-DR, HLA-ABC, CD14, CD31, CD34, CD44, CD49d, CD49e, CD73, CD79, CD90, CD105, CD166 and anti-human APC conjugated antibodies against CD45 (BD Biosciences) for 30 min. Samples were analyzed using a FACScalibur flow cytometer (Becton Dickinson), and data acquired were analyzed using WinMDI 2.8 software (Scripps Institute, La Jolla, CA). For differentiation, hMSCs were plated on 24 well plates at 5×10^4 cells/cm^2. Osteogenic differentiation medium consists of DMEM low glucose, 10% FBS, 10 μg/mL insulin, 50 μg/mL ascorbic acid, 100 nM dexamethasone and 10 mM Na β-glycerophosphate. Differentiation was allowed for a period of 28 days. Detection of calcified areas was carried out by the Von Kossa method. Adipogenic differentiation was performed in DMEM low glucose, 10% FBS, 10 μg/mL insulin, 0.5 μM hydrocortisone, 0.5 μM isobutylmethylxanthine (IBMX), and 60 μM indomethacin. Differentiation protocol lasts 28 days, alternating 3 rounds of resting periods (growing the cells with DMEM low glucose and 20% FBS). Differentiation was revealed with oil red for the detection of lipid-containing drops. Chondrogenic differentiation medium consists of DMEM high glucose, 10% FBS, 50 μg/mL ascorbic acid, 100 nM dexametasone, 6.25 μg/mL transferring, 6.25 μg/mL selenite, 5.33 μg/mL linoleic acid, 10 ng/mL TGF-β (Peprotech) and 1.25 μg/mL BSA. Differentiation was allowed for 21 days. Chondrogenic differentiation was detected by periodic acid−Schiff (PAS) staining, revealing neutral (magenta) and acidic (blue) mucopolysaccharides. All chemicals were from Sigma-Aldrich.

Human Samples and Tumor Conditioned Medium (TCM) Generation. Tumoral and nontumoral tissues were obtained at the time of surgical resection or liver transplantation at our institution (Austral Universitary Hospital, Pilar, Buenos Aires, Argentina). Informed consent was obtained from all patients. Necrotic tissue was removed with iris scissors, and tissue was

minced into pieces smaller than 1 mm^3. To obtain tumor conditioned medium (TCM), part of the minced fragments was transferred into a 24 well tissue culture plate (6 fragments/well) with 500 μL of DMEM (2 μmol/L glutamine, 100 U/mL penicillin, and 100 mg/mL streptomycin) with 0.05% BSA but without FBS. The supernatant was collected 24 h later and stored at −80 °C until use. From one sample, primary culture of the cells from HCC (HC-PT-5) and adjacent tissue (AT-PT-5) was established; part of the minced fragments was washed with Hanks balanced salt solution (Sigma-Aldrich) and subsequently digested with type IV collagenase (Calbiochem) for 1 h at 37 °C. The released cells were filtered through a 70 μm mesh (BD biosciences) to remove large debris fragments. Collagenase was removed by dilution with PBS before centrifugation for 5 min at 1500 rpm. Cells were washed twice with PBS and seeded (4×10^6 cells/cm^2) in 70% DMEM/30% F12 (Invitrogen/Life Technologies) complete culture medium supplemented with 8.5 ng/mL Cholera Toxin (Sigma-Aldrich), 10 ng/mL EGF (Prepotech), 1X ITS Liquid Media Supplement (Sigma-Aldrich), and 0.8 μg/mL hydrocortisone (Sigma-Aldrich). Cells were cultured until passage 5.

Animal Tumor and TCM. Lung, liver, spleen or tumors from male nude BALB/c mice with subcutaneous tumor (sc HuH7), orthotopic tumor (ih HuH7), fibrosis (TAA), orthotopic tumor associated to fibrosis or PBS (control) were obtained and processed as describe above for TCM.

Cell Conditioned Medium (CCM). Primary cultures and cell lines were plated as described above. After having reached 90% confluence, they were washed with PBS and cultured with DMEM (2 μmol/L glutamine, 100 U/mL penicillin, and 100 mg/mL streptomycin) without FBS. Eighteen hours later conditioned medium was harvested and stored at −80 °C until use.

Three-Dimensional Spheroids. Twenty-four-well tissue culture plates were coated with 2% agarose in PBS. A total of 1.5×10^5 HCC cells, 7.5×10^4 LX-2, and 7.5×10^4 HMEC-1 per spheroid were mixed in complete DMEM to obtain a single multicellular spheroid per well. For unicellular spheroids, 3×10^5 HCC cells were used. Seventy-five microliters of supernatant was carefully removed from each well every 2 days and replaced with fresh medium. Spheroids were cultured for 7 days and used for the corresponding assay. Viability above 75% was confirmed by Trypan blue exclusion test in all experiments.

***In Vitro* Migration and Invasion Assays.** The *in vitro* hMSC migratory capacity to different CCM, TCM or spheroids was assayed using a 48-Transwell microchemotaxis Boyden Chamber unit (Neuroprobe, Inc.). In brief, hMSCs (1.2×10^3 cells/well) were placed in the upper chamber of the Transwell unit, which was separated from the lower chamber by 8 μm pore polycarbonate filters (Nucleopore membrane, Neuroprobe). For the invasion assay the polycarbonate filters were previously incubated with 10 μg/mL fibronectin (Sigma-Aldrich) or 10 μg/mL type IV collagen (Sigma-Aldrich) for 18 h at 4 °C. CCM or spheroids were placed in the lower chamber of the Transwell unit. Transendothelial invasion assay was performed using 24-Transwell units with 8 μm pore polycarbonate filters (Falcon, BD Labware). Briefly, HMEC-1 cells (2×10^5) were seeded in the upper chamber of the Transwell unit and cultured for 1 day prior to the assay. Then, CCM were placed in the lower chamber and hMSCs (4.5×10^3 cells/well), previously stained with Hoechst 33258 (Sigma-Aldrich), were seeded in the upper chamber of the Transwell unit. All the systems were incubated for 4 or 18 h at 37 °C in a 5% CO_2 humidified atmosphere. After that, the membrane was carefully removed and cells on the upper side of the membrane were scraped off with a blade. Cells attached to the lower side of the membrane were fixed in 2% formaldehyde, and the membranes from the microchemotaxis Boyden Chamber unit were stained with 4′,6-diamidino-2-phenylindole dihydrochloride (DAPI, Sigma-Aldrich), except membranes from transendothelial invasion. Cells were counted using fluorescent-field microscopy and a 10× objective lens: the images captured in three representative visual fields were analyzed using CellProfiler software (www.cellprofiler.com), and the mean number of cells/field ± SEM was calculated. For blocking experiments, hMSCs were preincubated for 30 min with anti-CD49e or isotype control IgG1 (BD Biosciences) blocking antibodies at 20 times the saturating dilution as determined by flow cytometry prior to testing the potential involvement of these receptors in the invasion process. The TCM were incubated for 18 h at 37 °C in a 5% CO_2 humidified atmosphere.

Cell Adhesion Assays. For hMSC adhesion to endothelial cells, HMEC-1 cells (2×10^5) were seeded in a 96-well tissue culture plate and cultured for 1 day prior to assay. For cell adhesion to ECM components, 10 μg/mL fibronectin or 10 μg/mL type IV collagen was added to 96-well microplates and incubated at 4 °C overnight. After incubation, the wells were washed with PBS three times and blocked with 1% BSA in PBS at a 37 °C for 30 min. Coated wells were incubated for 5, 15, and 30 min with 5×10^3 cells of hMSC previously stained with *FAST*DiO (Molecular Probes), resuspended in different CCM or DMEM as control. The cell suspension was discarded, and the cells were fixed with 2% paraformaldehyde. The attached cells were visualized under a fluorescence microscope using a 20× objective lens. Images were captured and cells counted using the ImageJ software (National Institutes of Health, Bethesda, MD, USA). The results were plotted as *FAST*DiO relative area by normalizing values to those of hMSCs incubated with DMEM (control) for each time.

Gelatin Zymography Assay. To evaluate whether CCM induced gelatinolytic activity in hMSC supernatants, hMSCs (5×10^4) were seeded in 24-well plates for 18 h. Cells were treated with CCM or serum-free DMEM as untreated control for 6 h; hMSCs were then washed with PBS and cultured in DMEM for 6 h before supernatants were collected. MMP-2 activity was determined by zymography. Briefly, 40 μL of hMSC supernatant or CCM from HT-1080 (positive control) was run on a 10% SDS−PAGE containing 0.1% gelatin (Sigma-Aldrich). The gel was stained with Coomassie Brilliant Blue R-250 for 30 min at room temperature. Gelatinase activity was visualized by negative staining; gel images were obtained with a digital camera (Canon EOS 5D), and were subjected to densitometry analysis using Scion Image software (Scion Corporation, Frederick, MD). Relative MMP-2 activity was obtained by normalizing values to untreated samples (DMEM).

Proliferation Assays. Cells were seeded in 96-well culture tissue plates at 3×10^4cell/cm^2 density for 1 day prior to the assay. Then cells were cultured with CCM or complete DMEM as control for 48 h. Cell proliferation was evaluated by [^{3}H]-thymidine incorporation assay. Each sample was assayed in sextuplicate and normalized to control.

Mice and *in Vivo* Experiments. Six- to eight-week-old male nude BALB/c mice were purchased from CNEA (Comisión Nacional de Energía Atómica, Ezeiza, Buenos Aires, Argentina). Animals were maintained at our Animal Resources Facilities

(School of Biomedical Sciences, Austral University) in accordance with the experimental ethical committee and the NIH guidelines on the ethical use of animals. *Subcutaneous model*: HuH7 cells (2×10^6) were inoculated subcutaneously (sc) into the right flank of nude mice. *Orthotopic model with and without underlying fibrosis*: HuH7 cells (2×10^6) were inoculated directly into the liver by laparotomy in mice with or without fibrosis. Fibrosis was induced by ip administration of 0.15 mg/g body weight three times per week of thioacetamide (TAA, Sigma-Aldrich) for 6 weeks before tumor cell grafting. Control group inoculated with PBS and fibrosis group (TAA) were also included. To evaluate the effect of hMSC on tumor development, sc HuH7 tumors were established and after 10 days hMSC were iv injected. Tumor growth was assessed by caliper measurement, and tumor volume (mm^3) was calculated by the formula $\pi/6 \times$ larger diameter $\times$ (smaller diameter)^2. For *in vivo* migration studies, hMSCs were stained with CMDil for histological analysis and DiR (Molecular Probes, Invitrogen) for fluorescence imaging (FI). hMSCs (5×10^5) were intravenously (iv) injected 10 days after tumor inoculation. FI was performed using the Xenogen In Vivo Imaging System (IVIS; Caliper Life Sciences, Hopkinton, MA, USA). Mice injected with CMDiI-DiR-labeled hMSCs were analyzed at 1 h after hMSC injection and every day until the experimental end point. Images represent the radiant efficiency and were analyzed with IVIS Living Image (Caliper Life Sciences) software. Regions of interest (ROI) were manually drawn around the isolated organs to assess the fluorescence signal emitted. Results were expressed as total radiant efficiency in units of photons/second within the region of interest $[p/s]/[\mu W/cm^2]$.

Detection of hMSC by Fluorescence and Immunofluorescence Studies. To detect CMDiI+ cells within tissues, frozen sections were mounted in mounting media with DAPI (Vector Laboratories, Inc.) and observed under a fluorescence microscope using a 20× objective lens. Images were captured, cells were counted using the ImageJ software (National Institutes of Health, Bethesda, Maryland, USA) and the mean number of cells/field ± SEM was calculated. Immunofluorescence for von Willebrand factor and VCAM (CD106) were performed on frozen sections. After a 1 h incubation in blockage buffer (5% normal donkey serum, Jackson ImmunoResearch, PA, USA; 1% BSA, 0.3% Triton-X in PBS; room temperature), tissue was incubated overnight at 4 °C with a rabbit anti-von Willebrand factor polyclonal antibody (vWF; 1:215; Sigma, MO, USA) or a rat anti-mouse VCAM monoclonal antibody (1:25, BD Biosciences). After extensive washing, tissue was incubated with FITC-conjugated donkey anti-rabbit IgG or anti-rat IgG secondary antibodies (1:450 and 1:50 respectively; 2 h, room temperature; Vector Laboratories, Inc.). Slides were mounted in mounting media with DAPI (Vector Laboratories, Inc.) and analyzed under a fluorescence microscope. Control experiments without primary antibody showed only a faint background staining (not shown).

Statistical Analyses. One-way analysis of variance or Kruskal–Wallis and Dunn's post-tests (GraphPad Prism Software) were used for statistical analyses. Differences with p values lower than 0.05 were considered as statistically significant.

RESULTS

hMSC Characterization and Expression of Homing Receptors. Flow cytometry analysis indicated that hMSCs were positive for CD105, CD73, CD90, CD166 and HLA-ABC but negative for CD31, CD34, CD45, CD14, CD79 and HLA-DR markers (Supplementary Figure 1A in the Supporting Information). Additionally, hMSCs were found to differentiate into adipoblasts (oil-red-O staining), osteoblasts (Von Kossa staining) or chondroblasts (PAS staining) when subjected to appropriate differentiation assays (data not shown). These findings are in accordance with the International Society for Cellular Therapy (ISCT) criteria for defining MSCs.[27] Moreover, hMSCs also expressed high levels of adhesion receptors such as CD44 (96.8 ± 2.9) and α5 integrin (96.2 ± 2.1), and low levels of α4 integrin (14.5 ± 4.6) (Supplementary Figure 1B in the Supporting Information).

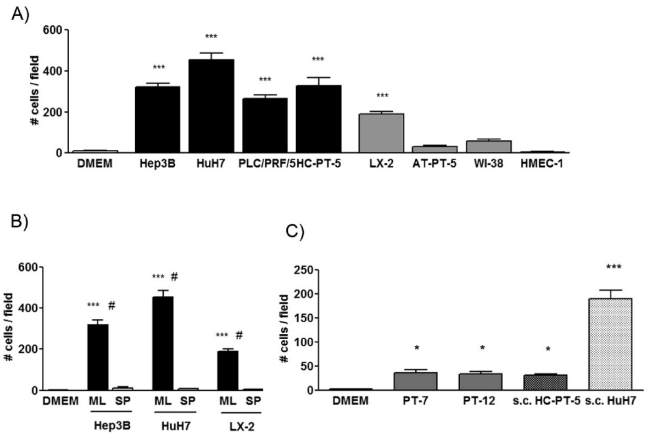

Figure 1. *In vitro* migration of hMSCs. (A) Migration of hMSCs toward CCM of human HCC cell lines (Hep3B, HuH7, PLC/PRF/5), primary culture from a HCC patient (HC-PT-5), human HSC cell line (LX-2), primary culture of nontumoral tissue from a HCC patient (AT-PT-5), fibroblasts (WI-38), endothelial cells (HMEC-1), or DMEM. $^{***}p < 0.001$ vs DMEM. (B) Migration of hMSCs toward CCM from monolayer (ML) or spheroid (SP) cultures from Hep3B, HuH7 or LX-2. $^{***}p < 0.001$ vs DMEM and $^{\#}p < 0.01$ vs SP. (C) Migration of hMSCs toward TCM from fresh HCC samples (PT-7 and PT-12) or from sc HC-PT-5 or HuH7 tumors established in BALB/c nude mice. $^{***}p < 0.001$ and $^{*}p < 0.05$ vs DMEM. Bars represent the average of hMSCs/field (10×) ± SEM from three representative visual fields. Results are representative of 4 independent experiments.

hMSCs Migrate toward Tumor and Hepatic Stellate Cells (HSCs) Conditioned Media. Our first aim was to evaluate migration capacity of hMSCs toward CMM derived from HCC cell lines. For this purpose a 4 h migration was assay in a modified Boyden chamber. Cells were allowed to migrate toward with CCM from established HCC cell lines (Hep3B, HuH7 and PLC/PRF/5), a primary culture from a HCC patient (HC-PT-5), as source of chemoattractants, or DMEM as control. An increase in the migratory capacity of hMSCs toward all HCC CCM was found when compared to DMEM (Figure 1A).

We next wondered whether hMSCs migration could be influenced by factors produced by tumor stroma. For this purpose, migration was evaluated using CCM from HSCs (LX-2 cell line), primary culture of cells obtained from the nontumoral tissue from a HCC patient (AT-PT-5), fibroblasts (WI-38 cell line) and endothelial cells (HMEC-1 cell line). From all conditions analyzed only CCM generated from LX-2 cells had the ability to induce significant migration of hMSCs (Figure 1A).

The above results were obtained using CCM derived from cells cultured as monolayer. We next decided to evaluate whether CCM from spheroid cultures could also induce hMSC migration.

Surprisingly, CCM derived from spheroids composed only of HCC cell lines did not induce hMSC migration (Figure 1B). Similarly, CCM obtained from multicellular spheroids composed of HCC cells, HSCs and HMEC-1 cells were unable to induce hMSC migration, even after 18 h incubation (data not shown).

Considering that CMM from HCC cell lines cultured as monolayer were able to induce migration of hMSCs but the same cells cultured as spheroids were not, we next asked whether conditioned media generated from HCC tumors (TCM) might contain chemoattractant properties for hMSCs. For that purpose, TCM were obtained from fresh HCC samples and from sc tumors induced by application of HC-PT-5 or HuH7 cells in BALB/c nude mice. Tumors were minced into small pieces and incubated in DMEM for 24 h to obtain TCM. HuH7 TCM was found to induce hMSC migration (~190 cells/field) but in a lesser amount than HuH7 CCM (~450 cells/field). Interestingly, TCM from fresh human samples (PT-7 and PT-12) and from sc tumor generated from a primary culture of the cells obtained from a patient with HCC (HC-PT-5) induced hMSC migration, although to a lesser extent than HuH7 TCM (Figure 1C).

CCM Increased Adhesion and Invasion Capacity of hMSCs. Arrest of hMSCs within tumor vasculature and subsequent transmigration across the endothelium are necessary events for an efficient homing of these cells into tumor tissue. Therefore, we decided to study hMSC ability to adhere to endothelial cells (HMEC-1), type IV collagen and fibronectin. After 30 min of exposure to CCM derived from HCC or LX-2 cells, a significantly increased adhesion of hMSCs to endothelial cells was found when compared to DMEM alone (Figure 2A). This was also the case when cells were placed into type IV collagen and fibronectin coated surfaces for 5 min (Figure 2B,C). This capacity to adhere to ECM is likely transient since after 15 or 30 min no differences were found when compared to control condition (DMEM).

To further characterize the effect of CCM on hMSCs, we decided to evaluate their invasive capacity using a Transwell two-chamber system in which endothelial cells were seeded on the upper compartment, or this surface was coated with type IV collagen or fibronectin. All CCM were found to significantly increase invasion of hMSCs in the 3 conditions tested (Figure 3, panels A, B and C respectively). Interestingly, invasion to fibronectin was significantly reduced by pretreatment with anti-CD49e antibody, which inhibits $\alpha5\beta1$/ligand binding, when compared to controls (Figure 3C). These results suggest that $\alpha5\beta1$ integrins are likely involved in hMSC invasiveness to fibronectin. Metalloproteinases (MMPs) are enzymes mediating cell invasiveness through the ECM. In order to evaluate MMP activity in hMSCs, zymograms were performed. Exposure of hMSCs to CCM from HCC and HSC cell lines was found to induce MMP-2 but not MMP-9 activity when compared to DMEM alone (Figure 3D).

Proliferation of hMSC and Tumor Cells. It is known that hMSCs and tumor cells produce several factors that are involved in cell proliferation. Thus, we next decided to evaluate whether factors produced by HCC cells or HSCs might influence hMSC

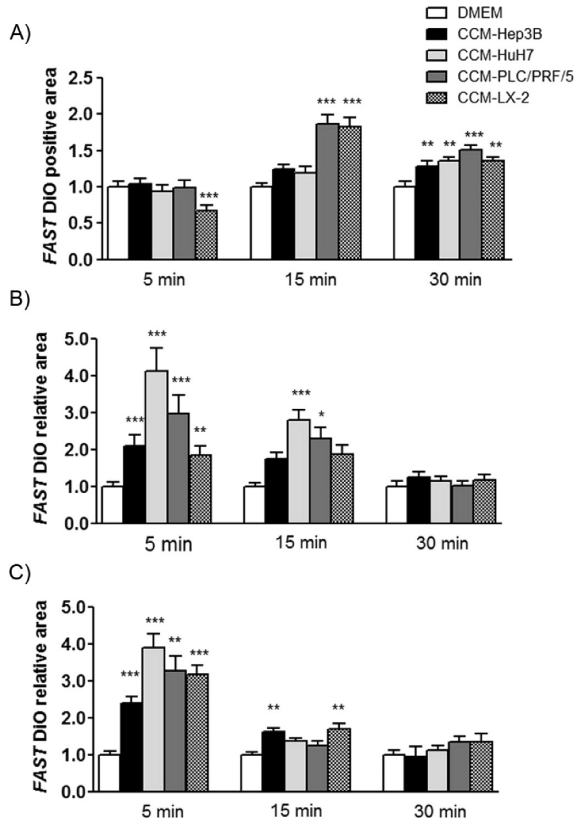

Figure 2. *In vitro* adhesion of hMSCs to endothelial cells (A), type IV collagen (B) and fibronectin (C) after 5, 15, and 30 min of exposure to CCM from HCC and HSC cell lines or DMEM. The results are plotted as *FAST*DiO relative area by normalizing to hMSCs incubated with DMEM (control) for each time. Results are representative of 3 independent experiments. ***$p < 0.001$, **$p < 0.01$ and *$p < 0.05$ vs DMEM.

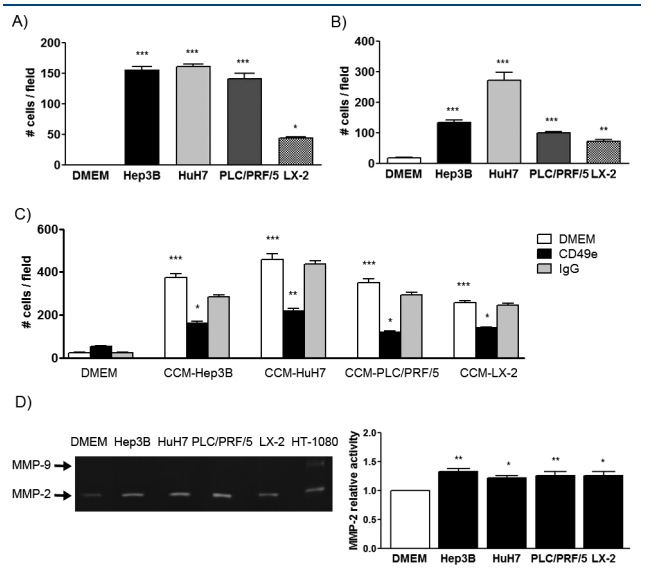

Figure 3. Cell conditioned medium from HCC and HSC cell lines induced *in vitro* invasion of hMSCs to endothelial cells (A) and type IV collagen (B). (C) hMSC invasion capacity to fibronectin using CCM from HCC and HSC cell lines or DMEM as chemoattractants (white bars), inhibition of $\alpha5\beta1$/ligand binding with anti-CD49e antibody (black bars) and isotype IgG (gray bars). Bars represent the average of hMSCs/field (10×) ± SEM from three representative visual fields. ***$p < 0.001$ vs DMEM. Results are representative of 3 independent experiments. **$p < 0.01$ and *$p < 0.05$ vs control (without pretreatment and isotype IgG). (D) MMP-2 activity was evaluated in supernatants of hMSCs after exposure to CCM from HCC and HSC cell lines by zymography. HT-1080 cell line was used as positive control. One representative zymogram is shown. Band intensity of 3 independent experiments was detected by densitometric evaluation and plotted as MMP-2 relative activity. **$p < 0.01$ and *$p < 0.05$ vs DMEM.

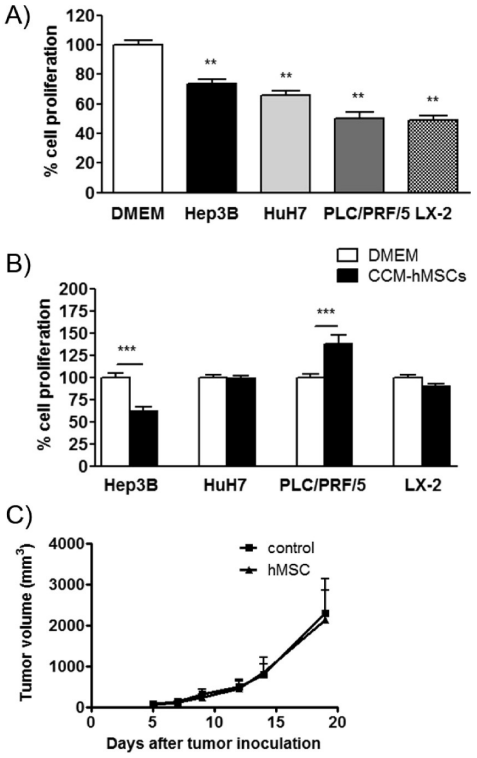

Figure 4. *In vitro* proliferation of hMSCs after exposure to CCM from HCC and HSCs or DMEM (A) and HCC cell line proliferation after exposure to hMSCs CCM or DMEM (B). Cell proliferation was evaluated by ^{3}H-thymidine incorporation assay at 48 h, and data are expressed as % cell proliferation relative to DMEM (100%) from 3 independent experiments. $^{**}p < 0.01$ vs DMEM. (C) Tumor volume measurements of HuH7 cells injected sc into BALB/c nude mice that received hMSC or saline (control). Data are expressed as mean tumor volume ± SEM.

proliferation and *vice versa*. For this purpose, *in vitro* hMSC proliferation was evaluated after 48 h of exposure with CCM from HCC cells and HSCs. All CCM were shown to decrease hMSC proliferation when compared to DMEM alone (Figure 4A). Interestingly, CCM from hMSCs had a heterogeneous effect on tumor cell proliferation and did not affect this behavior in LX-2 cells. While CCM from hMSCs did not modify HuH7 proliferation, this property was inhibited in Hep3B and enhanced in PLC/PRF/5 cells (Figure 4B).

We next decided to evaluate the effect of hMSC on tumor growth *in vivo*. For this purpose sc HuH7 tumors were established in BALB/c nude mice and, 10 days later, hMSCs were iv injected. Importantly, we did not observe any significant difference in HCC tumor growth after the administration of hMSCs in comparison with nontreated tumor bearing mice (Figure 4 C).

***In Vivo* Biodistribution of hMSCs in Tumor Bearing Mice.** We then evaluated the *in vivo* distribution of hMSCs after iv injection by fluorescence imaging (FI). For this purpose, hMSCs were stained with an infrared dye (DiR) and iv infused in sc HuH7 or ih HuH7 tumor bearing mice, fibrotic mice (TAA), ih HuH7 associated with fibrosis (TAA/ih HuH7) or control mice. Fibrosis was induced in BALB/c mice for 6 weeks achieving a F2−F3 stage (Supplementary Figure 2 in the Supporting Information) according to Metavir or Ishak scoring systems.[28] As it has been previously described, hMSCs were first trapped in the lungs, and then migrated to the liver and spleen, reaching the highest levels at day 3 (Supplementary Figure 3A in the Supporting Information). At day 7, mice were sacrificed and the strongest signal was observed in the liver, followed by spleen and lungs (Figure 5A). We analyzed the fluorescence signal in the isolated organs and found that in spleen and lung the signal was low and similar in all the studied groups. Regarding the analysis of the livers it was observed that the highest signals were achieved in fibrotic livers (TAA) and in ih HuH7-tumor bearing mice associated with fibrosis (TAA/ih HuH7) (Figure 5B). We also

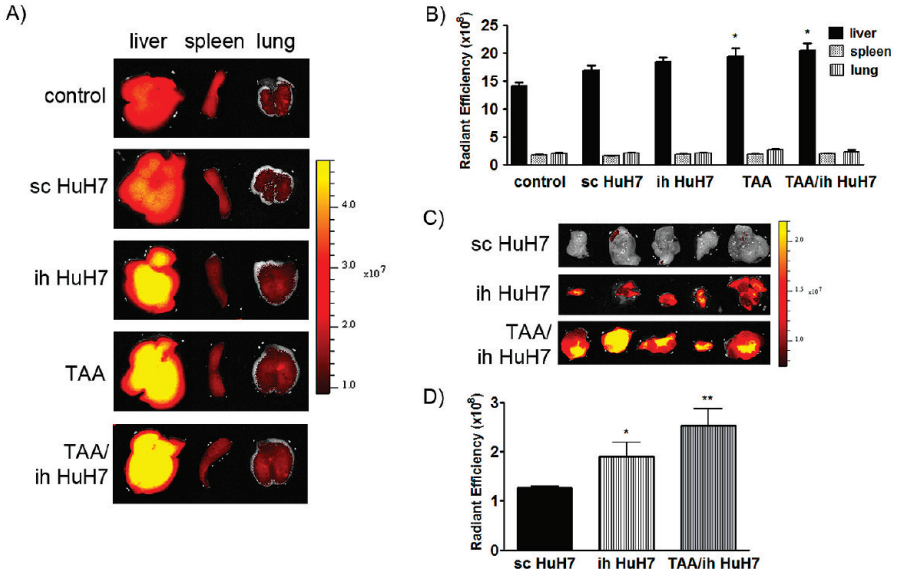

Figure 5. *In vivo* noninvasive biodistribution of hMSCs. DiR-labeled hMSCs were iv administered and monitored at 1 h, 3 days and 7 days after hMSC infusion in healthy mice (control) sc HuH7- and orthotopic HuH7-tumor bearing mice, fibrotic mice (TAA) and ih HuH7-tumor bearing mice with underlying fibrosis (TAA/ih HuH7). (A) At 7 days the tissues were removed and lungs, liver and spleen or tumors (C) were exposed to FI. Images represent the radiant efficiency. One representative image of 7 mice is shown. Regions of interest (ROI) calculated for the isolated liver, spleen and lung (B) and tumors (D) and results were expressed as total radiant efficiency ([p/s]/[μW/cm^2]). $^{*}p < 0.05$ vs control (B) and $^{**}p < 0.01$ and $^{*}p < 0.05$ vs sc HuH7 (D).

dx.doi.org/10.1021/mp200137c |*Mol. Pharmaceutics* 2011, 8, 1538–1548

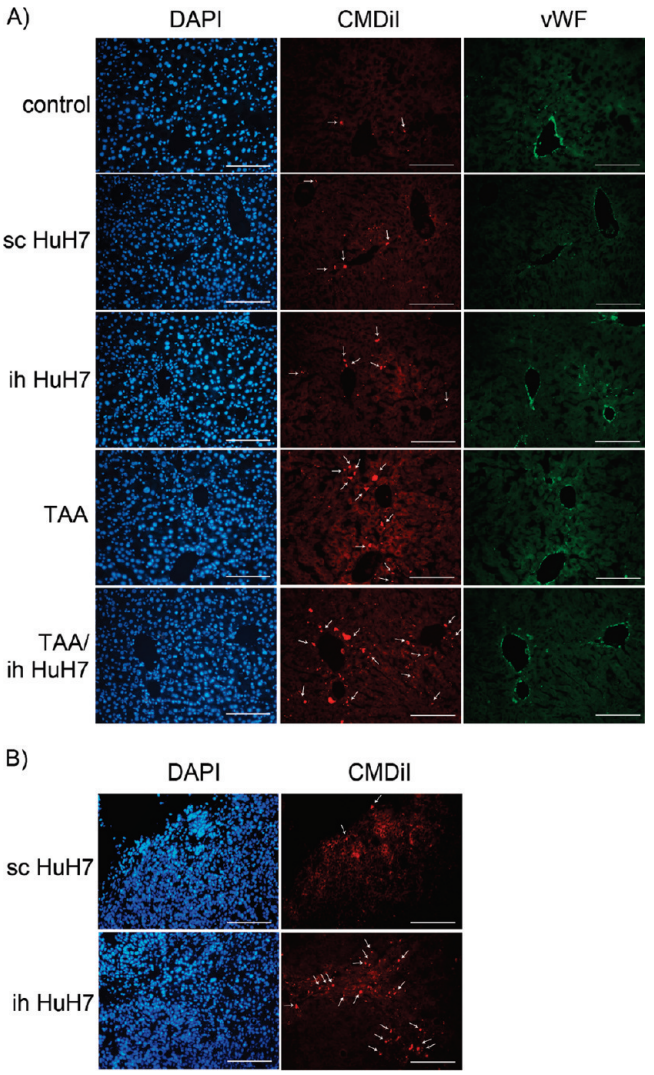

Figure 6. Microscopic localization of infused hMSCs. (A) Microscopic analysis of transplanted CMDiI-labeled hMSCs in livers of healthy mice (control), sc HuH7-tumor bearing mice, orthotopic HuH7-tumor bearing mice (ih HuH7), fibrotic mice (TAA) and orthotopic HuH7 associated to fibrosis (TAA/ih HuH7). CMDiI-labeled hMSCs (red signal, indicated by arrows) and DAPI staining were visualized in frozen sections from liver. Endothelial cells were visualized by von Willebrand factor staining (vWF). (B) Microscopic analysis CMDiI-labeled hMSCs (red signal, indicated by arrows) in sc HuH7 and ih HuH7 tumors. Scale bar = 50 μm.

observed hMSCs within tumors finding higher signal in orthotopic tumors associated or not with fibrosis (ih HuH7) than in sc tumors (Figure 5C,D). Although expected, it is worth noting that ih HuH7 tumor volume was significantly higher in mice with fibrosis than in mice without fibrosis (Supplementary Figure 3B in the Supporting Information). To further validate FI measurements, tissues were sectioned and the presence of CMDiI+ cells was evaluated by fluorescence microscopy. In the liver, hMSCs were preferentially found in a perivascular localization (Figure 6A). Quantification of CMDiI+ cells in the liver by fluorescence microscopy demonstrated that tumor bearing mice and fibrotic mice have more CMDiI+ cells than control group (Figure 7A). Moreover TAA and TAA/ih HuH7 mice have significantly more CMDiI+ cells in the liver than sc HuH7 and ih

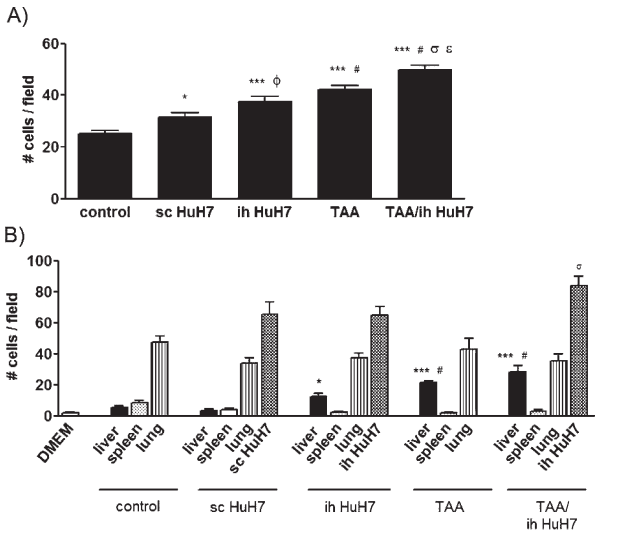

Figure 7. (A) Quantification of CMDiI+ cells by fluorescence microscope in liver sections of all the experimental groups. Bars represent the average of hMSCs/field (20×) ± SEM from ten representative visual fields. ***$p < 0.001$ and *$p < 0.05$ vs control mice, $^{\#}p < 0.01$ vs sc Huh7, $^{\phi}p < 0.05$ vs sc HuH7, $^{\varepsilon}p < 0.01$ vs ih HuH7 and $^{\sigma}p < 0.05$ vs TAA mice. (B) *In vitro* migration of hMSCs to TCM derived from different organs removed from healthy (control), sc HuH7- and ih HuH7-tumor bearing, fibrotic mice (TAA) and ih HuH7-tumor bearing associated with fibrosis (TAA/ih HuH7). Bars represent the average of hMSCs/field (10×) ± SEM from three representative visual fields. Results are representative of 3 independent experiments. ***$p < 0.001$ and *$p < 0.05$ vs liver of control and sc HuH7-tumor bearing mice and $^{\#}p < 0.05$ vs liver of ih HuH7-tumor bearing mice and $^{\#}p < 0.05$ vs sc and ih HuH7-tumor bearing mice.

HuH7 groups. In addition, ih HuH7 group has more CMDiI+ cells than sc HuH7 group (Figure 7A). The presence of CMDiI+ cells within the tumors was also analyzed by fluorescence microscopy. We observed a higher amount of hMSC inside ih HuH7 tumors in comparison with sc tumors as it was previously observed by FI (Figure 6B).

Taking into account that hMSCs were also observed in lungs and spleens we decided to analyze whether these tissues produce factors that might induce hMSC migration or anchor due to circulation or tissue anatomy features. For this purpose, livers, spleens, lungs and tumors were removed from all the experimental groups and TCM was obtained from these samples. *In vitro* migration of hMSC toward TCM obtained from tumors (sc or ih) was significantly higher than to TCM obtained from liver, spleen or lung (Figure 7B). TCM obtained from TAA/ih HuH7 tumors induced higher migration than ih and sc HuH7 tumors. TCM obtained from liver from ih HuH7, TAA and TAA/ih HuH7 mice induced higher hMSC migration than TCM obtained from liver from control and sc HuH7 mice (Figure 7B). Moreover, TCM obtained from livers of TAA and TAA/ih HuH7 mice induced a significantly higher migration of hMSC when compared to those obtained from ih HuH7 mice. Migration of hMSC toward TCM generated from lungs and spleens was similar in all the experimental groups (Figure 7B).

In order to find a possible mechanism involved in hMSC migration toward the injured livers and HCC tumors, we evaluated VCAM-1 expression in all experimental groups. Immunofluorescence demonstrated that the expression of VCAM-1

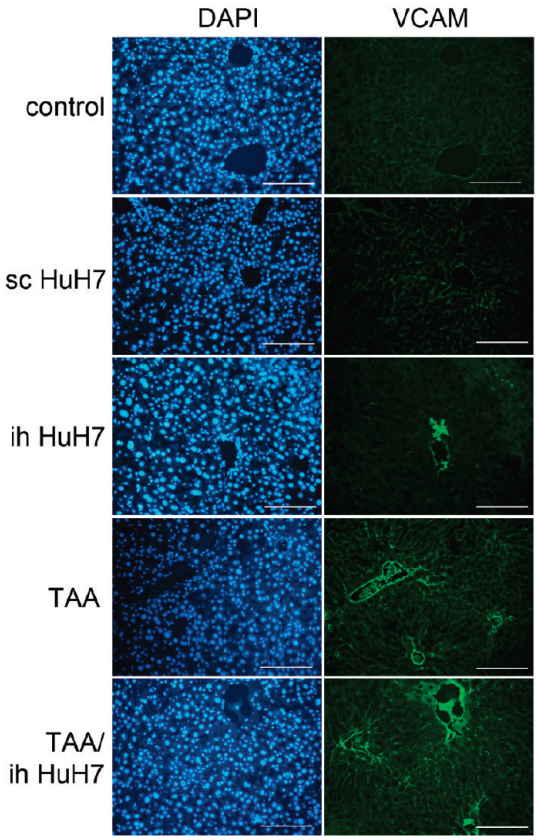

Figure 8. VCAM expression was visualized in frozen sections from liver of healthy (control), sc HuH7- and ih HuH7-tumor bearing, fibrotic mice (TAA) and ih HuH7-tumor bearing mice associated with fibrosis (TAA/ih HuH7). Scale bar = 50 μm.

was significantly increased in fibrotic livers as well as in orthotopic HCC tumors associated with fibrosis in comparison with controls (Figure 8).

DISCUSSION

MSCs are regarded as promising cell carriers for delivery of antitumoral genes to tumors without damaging nontumoral parenchyma.[29] These cells were previously found to migrate toward factors released by melanoma, breast cancer, glioma, prostate and colorectal carcinoma cell lines.[6,11,30,31] In addition, Gao et al. have recently described hMSC migration toward HCC.[32] We herein show that hMSCs respond to factors produced by HCC tumor cell and HSC lines and for the first time by fresh HCC tumor samples by increasing their migration toward their source, both *in vivo* and *in vitro*. In contrast, hMSC showed limited migration toward fibroblasts, endothelial cells or primary cultures from nontumoral adjacent tissue. These results are consistent with previous reports showing that MSC migration is restricted to tumor with little recruitment to nontumoral parenchyma.[29]

It is worth noting that migration of hMSCs was not induced by CCM generated from spheroids. It has been recently shown that the HCC cell line HepG2 substantially changes their gene expression pattern depending on the physical structure of the cells.[33] In this sense, cells in monolayer expressed high levels of genes related to ECM, cytoskeleton and adhesion molecules, whereas spheroids upregulated metabolic and synthetic functional genes.[33] In contrast, hMSCs migrated toward glioma[10] and pancreatic tumor cell[34] spheroids, and in human ovarian cancer cell lines, vascular endothelial growth factor A (VEGF-A) expression was higher during growth as a multicellular spheroid compared to monolayer culture.[35] Our results also demonstrated that TCM from fresh human HCC or sc tumors generated in nude mice from a primary human HCC cell culture or from HuH7 human cell line induce hMSC migration but to a lesser extent than CCM. These results are in line with the previous one where CM from spheroids did not induce hMSC migration, indicating that tumor cell lines respond with different genetic programs depending on the physical environment of 2D or 3D culture, and the gene expression pattern seems to differ between tumor types. This data result of interest and suggest that *in vitro* migration could be useful to study mechanisms involved in this process, but when cells achieve a 3D structure, HCC cells possibly downregulate genes related to adhesion and migration that could explain the less extent of hMSC migration observed *in vivo*. In addition, TCM from fresh HCC samples and from sc tumor generated by a primary culture of human HCC were shown to induce hMSC migration, although to a lesser extent than TCM from HuH7 sc tumors. This is consistent with previous reports showing that application of new anticancer drugs to established cell lines does not frequently correlate with clinical outcome, while primary tumor cultures do it better.[36] Thus, our results support the use of fresh samples or primary cultures as accurate models to mimic tumor behavior in patients and in experimental models.

Several chemotactic factors have demonstrated capacity to induce hMSC migration both *in vitro* and *in vivo*; among them stromal-derived factor 1 (SDF-1), basic fibroblast growth factor (bFGF), and vascular endothelial growth factor A (VEGF-A) have been extensively estudied.[37−39] It is known that HCC produces several cytokines and chemokines such as IL-6, IL-8, IL-10, IFN-γ, VEGF, HGF, and IGF-1.[19,20,23] The majority of them showed ability to induce hMSC migration,[24] but whether these or other chemoattractant factors are involved in the migratory behavior of hMSCs toward HCC remain to be elucidated.

Systemic infusion of MSCs is the most feasible and explored way of administration. For this delivery route to be successful it is mandatory that MSCs transmigrate across the endothelium and invade their target tissue. Previous reports indicated that MSC adhesion[40−42] and transmigration[43] through endothelial cells involve VLA-4/VCAM-1axis. Our results indicate that exposure of hMSC to CCM from HCC cell lines and HSCs was able to enhance their *in vitro* adhesion capacity to components of the vasculature such as endothelial cells and type IV collagen as well as to the ECM protein fibronectin. Moreover, pretreatment of these cells with the CCM resulted in increased invasion capacity to fibronectin, type IV collagen and endothelial barrier. In leukocytes, $\alpha5\beta1$ integrin (CD49e/CD29) selectively recognizes fibronectin and mediates cell migration;[44] we additionally demonstrated that application of anti-CD49e antibody that blocks $\alpha5\beta1$ integrins significantly reduced the invasion of CCM-treated cells to fibronectin was significantly reduced, strongly suggesting their involvement in HCC-mediated hMSC invasion.

Metalloproteinases are necessary for transmigration over the endothelial barrier. We have herein shown that exposure of hMSC to CCM from HCC cells and HSCs induced MMP-2 but not MMP-9 activity in hMSCs. Our results are in agreement with previous data indicating that MMP-2 but not MMP-9 mRNA and gelatinase activity were found in hMSC.[37] MMP-2 activity of hMSCs was previously shown to be increased after exposure to

inflammatory cytokines[45] and its inhibition was able to reduce transendothelial migration capacity of these cells.[46,47]

Once hMSCs are recruited to tumors, cancer cells can modulate hMSC behavior; MSC, in turn, can also regulate tumor proliferation through the secretion of different growth factors, chemokines and cytokines.[48] Our results indicate that CCM from HCC cells and HSCs inhibited hMSC proliferation *in vitro* likely involving several tumor derived factors. In fact, it was previously shown that hepatocyte growth factor (HGF) is able to inhibit MSC proliferation by inducing cell arrest in the G1-S checkpoint, as well as by inducing cytoskeletal rearrangements and cell migratory capacity.[49] It has also been described that TGF-β inhibits the growth of hematopoietic, epithelial, and endothelial cells.[50] Moreover, during *in vitro* culture, hMSCs increased TGF-β1 and TGF-β2 secretion and these cytokines probably act by an autocrine manner repressing the c-myc transcriptional activity via Smad3 and thereby arresting cell cycle and inhibiting MSC growth.[51] In addition, TGF-β is a well-known profibrogenic cytokine, produced by LX-2 cells.[52] These factors as well as others might be involved in the observed *in vitro* inhibition of hMSC proliferation.

Taking into account that one of the key functions of MSCs is to participate in wound healing, secretion of several cytokines and matrix proteins, stimulation of endothelial cells proliferation to support vasculogenesis and angiogenesis, and immunosupresive effects are effects that MSC may produce once they arrive in the tumor microenvironment.[53] We observed that factors produced by hMSCs have different effects on HCC and HSC proliferation. Thus, CCM generated from hMSCs induced the proliferation of PLC/PRF/5 cells, whereas this process was inhibited in Hep3B cells or was unaffected in HuH7 and LX-2 cells. These results are somehow expected considering that this issue remains controversial: a number of articles show opposite role of MSCs in tumor growth, and several approaches have been conducted to decipher whether MSC suppress or stimulate tumor growth.[54] Particularly in HCC, the available literature suggest that hMSCs are able to inhibit tumor growth.[55,56] However, a recent study indicated that hMSCs enhance proliferation of HCC cells *in vitro* and *in vivo* but reduced tumor cell invasiveness and lung metastasis through regulation of TGF-β1 production.[57] Consistent with the lack of effect of hMSC on HuH7 proliferation *in vitro*, we observed that systemic administration of hMSC in a subcutaneous model of HuH7 did not modify tumor growth *in vivo*. These results allow us to use HuH7 cells for *in vivo* studies, and, considering the potential therapeutic use of MSCs against tumors, MSC engineered to produce antitumoral proteins is still an attractive strategy to be considered for future clinical development.

Several reports described MSC distribution *in vivo*, and the majority of them indicated that iv injected hMSCs were detected primarily in the lungs and then secondarily in the liver and other organs.[58,59] Similar results were observed in all the experimental groups: when hMSC were systemically administered, a weak signal was observed in lungs and liver during the first hours but increasing at day 3. Seven days after hMSCs inoculation, infused cells were found principally in the liver, but the intensity of the signal was different between the experimental groups. In fact, we observed that the mice with tumor (sc or ih) and/or fibrosis presented higher signal intensity corresponding to hMSC in comparison with control mice. Moreover, in fibrotic livers the signal of hMSC was increased compared with livers from sc HuH7-tumor bearing mice. We also observed that hMSC were located inside HCC tumor nodules, and, importantly, the amount of hMSC was superior within ih tumors compared with sc tumors. It has been previously described that only a small fraction of MSCs could be observed in the vicinity of sc tumors.[60] In our study, hMSC were found located principally at the edge of sc tumors at 7 days postinfusion, similarly to what Gao et al. recently described for sc HCC tumors.[32] Of note is that when orthotopic HuH7 tumors were established in fibrotic livers, hMSC were able to migrate more efficiently inside HCC tumors when compared with the migration toward HuH7 tumors established in noncirrhotic mice.

One possible mechanism involved in the *in vivo* recruitment of hMSC is the increased expression of VCAM-1 in the liver vasculature, which normally mediates cellular extravasation to sites of tissue inflammation.[61] We observed an increased VCAM expression in livers from sc HuH7-tumor bearing mice and to a greater extent in livers derived from TAA/ih HuH7 tumors. In line with this, it was previously reported that cancer cells that reach the liver induce the activation of sinusoidal endothelial cells and lead to secretion of several cytokines including TNF-α, IL-1, IL-18, VEGF and to upregulation of VCAM-1, ICAM-1, P-selectin and E-selectin adhesion molecules.[62] Moreover, during the inflammatory process triggered by fibrotic stimuli, a large amount of proinflammatory cytokines, chemokines, growth factors and adhesion molecules such as VCAM-1 was observed.[63] This proinflammatory activation of sinusoids by cancer cells, the chemoattractant factors produced during fibrogenesis and the upregulation of adhesion molecules such as VCAM-1 can explain, at least in part, the enhanced recruitment of hMSC in the livers of mice bearing tumors with fibrosis.

As expected TCM generated from sc HuH7 tumors as well as from orthotopic HuH7 tumors induced a significantly higher *in vitro* migratory capacity of hMSCs in comparison with TCM from liver, spleen or lungs. In addition, hMSCs engraftment into the sc HCC tumors was significantly reduced in comparison with ih tumor nodules perhaps due to the particular vascular anatomy of the liver and the different tissue microenvironment.

There are controversies on whether hMSCs actively home tissues or become passively entrapped in small-diameter blood vessels.[25,64] Although hMSC can be passively retained in the liver, spleen and lung of healthy animals, our results suggest that, in our orthotopic model of HCC established in fibrotic mice, hMSCs are actively recruited inside hepatic tumors by factors produced by the tumor microenvironment, activated sinusoidal and hepatic stellate cells.

Taken together, our results demonstrate that hMSCs specifically migrate to factors produced by HCC and activated HSCs *in vitro* and *in vivo*. Factors produced by HCC cells induced adhesion and invasion of hMSCs to endothelial and ECM components, necessary for tissue-specific extravasation and homing. Finally, hMSCs efficiently engraft to the tumor and liver in an orthotopic HCC model. A better understanding of the mechanisms involved in *in vivo* migration is still needed in order to use them as a therapeutic tool for the treatment of both advanced HCC and cirrhosis.

■ ASSOCIATED CONTENT

Supporting Information. Figures depicting characterization of hMSCs, fibrosis evaluation in liver tissue, and *in vivo* noninvasive biodistribution of hMSCs. This material is available free of charge via the Internet at http://pubs.acs.org.

AUTHOR INFORMATION

Corresponding Author

*Liver Unit, School of Medicine, Austral University, Av. Presidente Perón 1500, (B1629ODT) Derqui-Pilar, Buenos Aires, Argentina. Phone: +54-2322-482618. Fax: +54-2322-482204. E-mail: gmazzoli@cas.austral.edu.ar.

Author Contributions

§Both authors equally contributed to this work.

ACKNOWLEDGMENT

We gratefully thank Soledad Arregui and Guillermo Gastón for technical assistance and Dr. Scott Friedman for providing LX-2 cells. This work was supported by grants from Austral University and from Agencia Nacional de Promoción Científica y Tecnológica (PAE-PICT-2007-00082; PICT-2007-00736; PICTO-AUSTRAL 2008-000115)

ABBREVIATIONS USED

CCM, cell conditioned media; HSCs, hepatic stellate cells; FI, fluorescence imaging; HCC, hepatocellular carcinoma; hMSCs, human mesenchymal stromal cells; ih, intrahepatic; sc, subcutaneous; TAA, thioacetamide; TCM, tissue conditioned media

REFERENCES

(1) El-Serag, H. B.; Marrero, J. A.; Rudolph, L.; Reddy, K. R. Diagnosis and treatment of hepatocellular carcinoma. *Gastroenterology* **2008**, *134* (6), 1752–63.

(2) Perz, J. F.; Armstrong, G. L.; Farrington, L. A.; Hutin, Y. J.; Bell, B. P. The contributions of hepatitis B virus and hepatitis C virus infections to cirrhosis and primary liver cancer worldwide. *J. Hepatol.* **2006**, *45* (4), 529–38.

(3) Llovet, J. M.; Ricci, S.; Mazzaferro, V.; Hilgard, P.; Gane, E.; Blanc, J. F.; de Oliveira, A. C.; Santoro, A.; Raoul, J. L.; Forner, A.; Schwartz, M.; Porta, C.; Zeuzem, S.; Bolondi, L.; Greten, T. F.; Galle, P. R.; Seitz, J. F.; Borbath, I.; Haussinger, D.; Giannaris, T.; Shan, M.; Moscovici, M.; Voliotis, D.; Bruix, J. Sorafenib in advanced hepatocellular carcinoma. *N. Engl. J. Med.* **2008**, *359* (4), 378–90.

(4) Hernandez-Alcoceba, R.; Sangro, B.; Prieto, J. Gene therapy of liver cancer. *World J. Gastroenterol.* **2006**, *12* (38), 6085–97.

(5) Garcia-Gomez, I.; Elvira, G.; Zapata, A. G.; Lamana, M. L.; Ramirez, M.; Castro, J. G.; Arranz, M. G.; Vicente, A.; Bueren, J.; Garcia-Olmo, D. Mesenchymal stem cells: biological properties and clinical applications. *Expert Opin. Biol. Ther.* **2010**, *10* (10), 1453–68.

(6) Studeny, M.; Marini, F. C.; Champlin, R. E.; Zompetta, C.; Fidler, I. J.; Andreeff, M. Bone marrow-derived mesenchymal stem cells as vehicles for interferon-beta delivery into tumors. *Cancer Res.* **2002**, *62* (13), 3603–8.

(7) Komarova, S.; Kawakami, Y.; Stoff-Khalili, M. A.; Curiel, D. T.; Pereboeva, L. Mesenchymal progenitor cells as cellular vehicles for delivery of oncolytic adenoviruses. *Mol. Cancer Ther.* **2006**, *5* (3), 755–66.

(8) Elzaouk, L.; Moelling, K.; Pavlovic, J. Anti-tumor activity of mesenchymal stem cells producing IL-12 in a mouse melanoma model. *Exp. Dermatol.* **2006**, *15* (11), 865–74.

(9) Deans, R. J.; Moseley, A. B. Mesenchymal stem cells: biology and potential clinical uses. *Exp. Hematol.* **2000**, *28* (8), 875–84.

(10) Schichor, C.; Birnbaum, T.; Etminan, N.; Schnell, O.; Grau, S.; Miebach, S.; Aboody, K.; Padovan, C.; Straube, A.; Tonn, J. C.; Goldbrunner, R. Vascular endothelial growth factor A contributes to glioma-induced migration of human marrow stromal cells (hMSC). *Exp. Neurol.* **2006**, *199* (2), 301–10.

(11) Hung, S. C.; Deng, W. P.; Yang, W. K.; Liu, R. S.; Lee, C. C.; Su, T. C.; Lin, R. J.; Yang, D. M.; Chang, C. W.; Chen, W. H.; Wei, H. J.; Gelovani, J. G. Mesenchymal stem cell targeting of microscopic tumors and tumor stroma development monitored by noninvasive in vivo positron emission tomography imaging. *Clin. Cancer Res.* **2005**, *11* (21), 7749–56.

(12) Kaplan, R. N.; Psaila, B.; Lyden, D. Niche-to-niche migration of bone-marrow-derived cells. *Trends Mol. Med.* **2007**, *13* (2), 72–81.

(13) Friedman, S. L. Mechanisms of hepatic fibrogenesis. *Gastroenterology* **2008**, *134* (6), 1655–69.

(14) Friedman, S. L. Liver fibrosis -- from bench to bedside. *J. Hepatol.* **2003**, *38* (Suppl 1), S38–53.

(15) Parola, M.; Robino, G. Oxidative stress-related molecules and liver fibrosis. *J. Hepatol.* **2001**, *35* (2), 297–306.

(16) Bataller, R.; Brenner, D. A. Liver fibrosis. *J. Clin. Invest.* **2005**, *115* (2), 209–18.

(17) Dvorak, H. F. Tumors: wounds that do not heal. Similarities between tumor stroma generation and wound healing. *N. Engl. J. Med.* **1986**, *315* (26), 1650–9.

(18) Mantovani, A.; Allavena, P.; Sica, A.; Balkwill, F. Cancer-related inflammation. *Nature* **2008**, *454* (7203), 436–44.

(19) Hsia, C. Y.; Huo, T. I.; Chiang, S. Y.; Lu, M. F.; Sun, C. L.; Wu, J. C.; Lee, P. C.; Chi, C. W.; Lui, W. Y.; Lee, S. D. Evaluation of interleukin-6, interleukin-10 and human hepatocyte growth factor as tumor markers for hepatocellular carcinoma. *Eur. J. Surg. Oncol.* **2007**, *33* (2), 208–12.

(20) Llovet, J. M.; Bruix, J. Molecular targeted therapies in hepatocellular carcinoma. *Hepatology* **2008**, *48* (4), 1312–27.

(21) Li, W.; Gomez, E.; Zhang, Z. Immunohistochemical expression of stromal cell-derived factor-1 (SDF-1) and CXCR4 ligand receptor system in hepatocellular carcinoma. *J. Exp. Clin. Cancer Res.* **2007**, *26* (4), 527–33.

(22) Rubie, C.; Frick, V. O.; Wagner, M.; Rau, B.; Weber, C.; Kruse, B.; Kempf, K.; Tilton, B.; Konig, J.; Schilling, M. Enhanced expression and clinical significance of CC-chemokine MIP-3 alpha in hepatocellular carcinoma. *Scand. J. Immunol.* **2006**, *63* (6), 468–77.

(23) Yamaguchi, R.; Yano, H.; Iemura, A.; Ogasawara, S.; Haramaki, M.; Kojiro, M. Expression of vascular endothelial growth factor in human hepatocellular carcinoma. *Hepatology* **1998**, *28* (1), 68–77.

(24) Spaeth, E.; Klopp, A.; Dembinski, J.; Andreeff, M.; Marini, F. Inflammation and tumor microenvironments: defining the migratory itinerary of mesenchymal stem cells. *Gene Ther.* **2008**, *15* (10), 730–8.

(25) Ley, K.; Laudanna, C.; Cybulsky, M. I.; Nourshargh, S. Getting to the site of inflammation: the leukocyte adhesion cascade updated. *Nat. Rev. Immunol.* **2007**, *7* (9), 678–89.

(26) Aquino, J. B.; Bolontrade, M. F.; Garcia, M. G.; Podhajcer, O. L.; Mazzolini, G. Mesenchymal stem cells as therapeutic tools and gene carriers in liver fibrosis and hepatocellular carcinoma. *Gene Ther.* **2010**, *17* (6), 692–708.

(27) Dominici, M.; Le Blanc, K.; Mueller, I.; Slaper-Cortenbach, I.; Marini, F.; Krause, D.; Deans, R.; Keating, A.; Prockop, D.; Horwitz, E. Minimal criteria for defining multipotent mesenchymal stromal cells. The International Society for Cellular Therapy position statement. *Cytotherapy* **2006**, *8* (4), 315–7.

(28) Poynard, T.; Bedossa, P.; Opolon, P. Natural history of liver fibrosis progression in patients with chronic hepatitis C. The OBSVIRC, METAVIR, CLINIVIR, and DOSVIRC groups. *Lancet* **1997**, *349* (9055), 825–32.

(29) Bexell, D.; Gunnarsson, S.; Tormin, A.; Darabi, A.; Gisselsson, D.; Roybon, L.; Scheding, S.; Bengzon, J. Bone marrow multipotent mesenchymal stroma cells act as pericyte-like migratory vehicles in experimental gliomas. *Mol. Ther.* **2009**, *17* (1), 183–90.

(30) Nakamizo, A.; Marini, F.; Amano, T.; Khan, A.; Studeny, M.; Gumin, J.; Chen, J.; Hentschel, S.; Vecil, G.; Dembinski, J.; Andreeff, M.; Lang, F. F. Human bone marrow-derived mesenchymal stem cells in the treatment of gliomas. *Cancer Res.* **2005**, *65* (8), 3307–18.

(31) Studeny, M.; Marini, F. C.; Dembinski, J. L.; Zompetta, C.; Cabreira-Hansen, M.; Bekele, B. N.; Champlin, R. E.; Andreeff, M. Mesenchymal stem cells: potential precursors for tumor stroma and targeted-delivery vehicles for anticancer agents. *J. Natl. Cancer Inst.* **2004**, *96* (21), 1593–603.

(32) Gao, Y.; Yao, A.; Zhang, W.; Lu, S.; Yu, Y.; Deng, L.; Yin, A.; Xia, Y.; Sun, B.; Wang, X. Human mesenchymal stem cells overexpressing pigment epithelium-derived factor inhibit hepatocellular carcinoma in nude mice. *Oncogene* **2010**, *29* (19), 2784–94.

(33) Chang, T. T.; Hughes-Fulford, M. Monolayer and spheroid culture of human liver hepatocellular carcinoma cell line cells demonstrate distinct global gene expression patterns and functional phenotypes. *Tissue Eng., Part A* **2009**, *15* (3), 559–67.

(34) Beckermann, B. M.; Kallifatidis, G.; Groth, A.; Frommhold, D.; Apel, A.; Mattern, J.; Salnikov, A. V.; Moldenhauer, G.; Wagner, W.; Diehlmann, A.; Saffrich, R.; Schubert, M.; Ho, A. D.; Giese, N.; Buchler, M. W.; Friess, H.; Buchler, P.; Herr, I. VEGF expression by mesenchymal stem cells contributes to angiogenesis in pancreatic carcinoma. *Br. J. Cancer* **2008**, *99* (4), 622–31.

(35) Sonoda, T.; Kobayashi, H.; Kaku, T.; Hirakawa, T.; Nakano, H. Expression of angiogenesis factors in monolayer culture, multicellular spheroid and in vivo transplanted tumor by human ovarian cancer cell lines. *Cancer Lett.* **2003**, *196* (2), 229–37.

(36) Cree, I. A.; Glaysher, S.; Harvey, A. L. Efficacy of anti-cancer agents in cell lines versus human primary tumour tissue. *Curr. Opin. Pharmacol.* **2010**, *10* (4), 375–9.

(37) Son, B. R.; Marquez-Curtis, L. A.; Kucia, M.; Wysoczynski, M.; Turner, A. R.; Ratajczak, J.; Ratajczak, M. Z.; Janowska-Wieczorek, A. Migration of bone marrow and cord blood mesenchymal stem cells in vitro is regulated by stromal-derived factor-1-CXCR4 and hepatocyte growth factor-c-met axes and involves matrix metalloproteinases. *Stem Cells* **2006**, *24* (5), 1254–64.

(38) Schmidt, A.; Ladage, D.; Schinkothe, T.; Klausmann, U.; Ulrichs, C.; Klinz, F. J.; Brixius, K.; Arnhold, S.; Desai, B.; Mehlhorn, U.; Schwinger, R. H.; Staib, P.; Addicks, K.; Bloch, W. Basic fibroblast growth factor controls migration in human mesenchymal stem cells. *Stem Cells* **2006**, *24* (7), 1750–8.

(39) Ji, J. F.; He, B. P.; Dheen, S. T.; Tay, S. S. Interactions of chemokines and chemokine receptors mediate the migration of mesenchymal stem cells to the impaired site in the brain after hypoglossal nerve injury. *Stem Cells* **2004**, *22* (3), 415–27.

(40) Segers, V. F.; Van Riet, I.; Andries, L. J.; Lemmens, K.; Demolder, M. J.; De Becker, A. J.; Kockx, M. M.; De Keulenaer, G. W. Mesenchymal stem cell adhesion to cardiac microvascular endothelium: activators and mechanisms. *Am. J. Physiol.* **2006**, *290* (4), H1370–7.

(41) Ruster, B.; Gottig, S.; Ludwig, R. J.; Bistrian, R.; Muller, S.; Seifried, E.; Gille, J.; Henschler, R. Mesenchymal stem cells display coordinated rolling and adhesion behavior on endothelial cells. *Blood* **2006**, *108* (12), 3938–44.

(42) Ip, J. E.; Wu, Y.; Huang, J.; Zhang, L.; Pratt, R. E.; Dzau, V. J. Mesenchymal stem cells use integrin beta1 not CXC chemokine receptor 4 for myocardial migration and engraftment. *Mol. Biol. Cell* **2007**, *18* (8), 2873–82.

(43) Steingen, C.; Brenig, F.; Baumgartner, L.; Schmidt, J.; Schmidt, A.; Bloch, W. Characterization of key mechanisms in transmigration and invasion of mesenchymal stem cells. *J. Mol. Cell. Cardiol.* **2008**, *44* (6), 1072–84.

(44) Jin, H.; Su, J.; Garmy-Susini, B.; Kleeman, J.; Varner, J. Integrin alpha4beta1 promotes monocyte trafficking and angiogenesis in tumors. *Cancer Res.* **2006**, *66* (4), 2146–52.

(45) Tondreau, T.; Meuleman, N.; Stamatopoulos, B.; De Bruyn, C.; Delforge, A.; Dejeneffe, M.; Martiat, P.; Bron, D.; Lagneaux, L. In vitro study of matrix metalloproteinase/tissue inhibitor of metalloproteinase production by mesenchymal stromal cells in response to inflammatory cytokines: the role of their migration in injured tissues. *Cytotherapy* **2009**, *11* (5), 559–69.

(46) De Becker, A.; Van Hummelen, P.; Bakkus, M.; Vande Broek, I.; De Wever, J.; De Waele, M.; Van Riet, I. Migration of culture-expanded human mesenchymal stem cells through bone marrow endothelium is regulated by matrix metalloproteinase-2 and tissue inhibitor of metalloproteinase-3. *Haematologica* **2007**, *92* (4), 440–9.

(47) Ries, C.; Egea, V.; Karow, M.; Kolb, H.; Jochum, M.; Neth, P. MMP-2, MT1-MMP, and TIMP-2 are essential for the invasive capacity of human mesenchymal stem cells: differential regulation by inflammatory cytokines. *Blood* **2007**, *109* (9), 4055–63.

(48) Littlepage, L. E.; Egeblad, M.; Werb, Z. Coevolution of cancer and stromal cellular responses. *Cancer Cell* **2005**, *7* (6), 499–500.

(49) Forte, G.; Minieri, M.; Cossa, P.; Antenucci, D.; Sala, M.; Gnocchi, V.; Fiaccavento, R.; Carotenuto, F.; De Vito, P.; Baldini, P. M.; Prat, M.; Di Nardo, P. Hepatocyte growth factor effects on mesenchymal stem cells: proliferation, migration, and differentiation. *Stem Cells* **2006**, *24* (1), 23–33.

(50) Tian, M.; Schiemann, W. P. The TGF-beta paradox in human cancer: an update. *Future Oncol.* **2009**, *5* (2), 259–71.

(51) Sawada, R.; Ito, T.; Tsuchiya, T. Changes in expression of genes related to cell proliferation in human mesenchymal stem cells during in vitro culture in comparison with cancer cells. *J. Artif. Organs* **2006**, *9* (3), 179–84.

(52) Camino, A. M.; Atorrasagasti, C.; Maccio, D.; Prada, F.; Salvatierra, E.; Rizzo, M.; Alaniz, L.; Aquino, J. B.; Podhajcer, O. L.; Silva, M.; Mazzolini, G. Adenovirus-mediated inhibition of SPARC attenuates liver fibrosis in rats. *J. Gene Med.* **2008**, *10* (9), 993–1004.

(53) English, K.; French, A.; Wood, K. J. Mesenchymal stromal cells: facilitators of successful transplantation? *Cell Stem Cell* **2010**, *7* (4), 431–42.

(54) Klopp, A. H.; Gupta, A.; Spaeth, E.; Andreeff, M.; Marini, F., 3rd. Concise review: dissecting a discrepancy in the literature: do mesenchymal stem cells support or suppress tumor growth? *Stem Cells* **2011**, *29* (1), 11–9.

(55) Qiao, L.; Xu, Z.; Zhao, T.; Zhao, Z.; Shi, M.; Zhao, R. C.; Ye, L.; Zhang, X. Suppression of tumorigenesis by human mesenchymal stem cells in a hepatoma model. *Cell Res.* **2008**, *18* (4), 500–7.

(56) Lu, Y. R.; Yuan, Y.; Wang, X. J.; Wei, L. L.; Chen, Y. N.; Cong, C.; Li, S. F.; Long, D.; Tan, W. D.; Mao, Y. Q.; Zhang, J.; Li, Y. P.; Cheng, J. Q. The growth inhibitory effect of mesenchymal stem cells on tumor cells in vitro and in vivo. *Cancer Biol. Ther.* **2008**, *7* (2), 245–51.

(57) Li, G. C.; Ye, Q. H.; Xue, Y. H.; Sun, H. J.; Zhou, H. J.; Ren, N.; Jia, H. L.; Shi, J.; Wu, J. C.; Dai, C.; Dong, Q. Z.; Qin, L. X. Human mesenchymal stem cells inhibit metastasis of a hepatocellular carcinoma model using the MHCC97-H cell line. *Cancer Sci.* **2010**, *101* (12), 2546–53.

(58) Gao, J.; Dennis, J. E.; Muzic, R. F.; Lundberg, M.; Caplan, A. I. The dynamic in vivo distribution of bone marrow-derived mesenchymal stem cells after infusion. *Cells Tissues Organs* **2001**, *169* (1), 12–20.

(59) Lee, R. H.; Pulin, A. A.; Seo, M. J.; Kota, D. J.; Ylostalo, J.; Larson, B. L.; Semprun-Prieto, L.; Delafontaine, P.; Prockop, D. J. Intravenous hMSCs improve myocardial infarction in mice because cells embolized in lung are activated to secrete the anti-inflammatory protein TSG-6. *Cell Stem Cell* **2009**, *5* (1), 54–63.

(60) Wang, H.; Cao, F.; De, A.; Cao, Y.; Contag, C.; Gambhir, S. S.; Wu, J. C.; Chen, X. Trafficking mesenchymal stem cell engraftment and differentiation in tumor-bearing mice by bioluminescence imaging. *Stem Cells* **2009**, *27* (7), 1548–58.

(61) Wu, T. C. The role of vascular cell adhesion molecule-1 in tumor immune evasion. *Cancer Res.* **2007**, *67* (13), 6003–6.

(62) Vidal-Vanaclocha, F. The prometastatic microenvironment of the liver. *Cancer Microenviron.* **2008**, *1* (1), 113–29.

(63) Sacanella, E.; Estruch, R. The effect of alcohol consumption on endothelial adhesion molecule expression. *Addict. Biol.* **2003**, *8* (4), 371–8.

(64) Sackstein, R.; Merzaban, J. S.; Cain, D. W.; Dagia, N. M.; Spencer, J. A.; Lin, C. P.; Wohlgemuth, R. Ex vivo glycan engineering of CD44 programs human multipotent mesenchymal stromal cell trafficking to bone. *Nat. Med.* **2008**, *14* (2), 181–7.